

EXTRACTING THE SHEAR RELAXATION TIME OF QUARK–GLUON PLASMA FROM RAPIDITY CORRELATIONS*

GEORGE MOSCHELLI

Lawrence Technological University
21000 West Ten Mile Road, Southfield, MI 48075, USA

SEAN GAVIN

Department of Physics and Astronomy, Wayne State University
Detroit, MI, 48202, USA

(Received April 11, 2019)

We propose that rapidity-dependent momentum correlations can be used to extract the shear relaxation time τ_π of the medium formed in high-energy nuclear collisions. Shear viscosity drives the initial fluctuations of the medium toward equilibrium at a rate characterized by the shear relaxation time. Momentum fluctuations, in excess of thermal fluctuations, that survive to freeze out, are remnants of the initial state, and influence the rapidity dependence of momentum correlations. We describe a method for calculating the rapidity dependence of two-particle momentum correlations with a second order, causal, diffusion equation that includes Langevin noise as a source of thermal fluctuations. In comparison to RHIC data, we find that the ratio $\tau_\pi/\nu \approx 5\text{--}6$, where $\nu = \eta/sT$ is the kinematic viscosity.

DOI:10.5506/APhysPolB.50.1139

1. Introduction

The medium produced in high-energy heavy-ion collisions is expected to rapidly reach a locally equilibrated quark–gluon plasma (QGP) state. However, at the onset of the formation of the QGP phase, the stress energy tensor describing energy and momentum densities is surely anisotropic over the collision volume and out of equilibrium. Hydrodynamics has been widely used to model the dynamics of the expansion and cooling of the system; viscous

* Presented at the Cracow Epiphany Conference on Advances in Heavy Ion Physics, Kraków, Poland, January 8–11 2019.

forces in hydrodynamic theories characterize the nature of the fundamental microscopic interactions that drive the system toward equilibrium. For this reason, experimental measurements of observables that are sensitive to viscous effects are critical for constraining these hydrodynamic theories. In addition to viscosity, these theories incorporate other such transport coefficients that similarly characterize the fundamental nature of the medium, but few have any experimental constraints.

We expand on our work [1] to propose a method for extracting another transport coefficient, the shear relaxation time τ_π , from the rapidity dependence of transverse momentum, p_t , correlations. In Sec. 2, we describe how correlations between momentum fluctuations are simultaneously driven toward an equilibrium state and also propagated through the medium by diffusion. The shear relaxation time characterizes the rate of isotropization of the medium due to shear viscous forces and, therefore, the rate at which correlations are transported through the medium. In particular, we focus on the spread of correlations in rapidity. In Sec. 3, we describe how these correlations are observable through the rapidity dependence of two-particle transverse momentum correlations, \mathcal{C} , and highlight the sensitivity of the data to τ_π . Finally, in Sec. 3.1, we describe how transport coefficients can be studied through moments of the rapidity distribution of \mathcal{C} .

2. Diffusion of momentum correlations

Correlations of momentum fluctuations are sensitive to both the so-called first and second order transport coefficients that characterize the dynamics of medium created in relativistic nuclear collisions. Relativistic hydrodynamics is often used to model the dynamics of these collisions and the equations of motion are determined by solving differential equations representing energy and momentum conservation, $\partial_\mu T^{\mu\nu} = 0$, and particle current conservation, $\partial_\mu J^\mu = 0$. Here, $T^{\mu\nu}$ is the stress energy tensor and J^μ is the particle current density. Schematically, including non-equilibrium motion amounts to adding source terms to the differential equations such that the stress-energy tensor and current density take forms such as $T^{\mu\nu} = T_{\text{ideal}}^{\mu\nu} + \Delta T^{\mu\nu}$ and $J^\mu = J_{\text{ideal}}^\mu + \Delta J^\mu$. The $\Delta T^{\mu\nu}$ and ΔJ^μ terms encompass effects from out-of-equilibrium dynamics due to shear and bulk viscosities, thermal conductivity, *etc.*

Transport coefficients like the shear and bulk viscosities show up in the so-called first order theories that have had success explaining dissipative dynamics. However, first order theories do not address the time scales over which dissipative forces transport correlation signals through the medium. Second order theories usually address this issue by utilizing a relaxation time approximation that enforces causality through the introduction of a relaxation time — a characteristic time that dictates the rate at which a

fluid approaches (local) equilibrium. Therefore, the shear relaxation time, τ_π , is as fundamentally important for characterizing the medium as is the shear viscosity itself.

The rapidity dependence of transverse momentum correlations is particularly sensitive to τ_π . Imagine two neighboring fluid cells with different transverse momenta. Shear viscosity acts between them such that the slower cell is sped up and the faster cell is slowed down, driving the two toward an average. In doing so, momentum is transferred in a direction that is perpendicular to the direction of the flow — in this case, in the longitudinal (rapidity) direction. Over time, fluid cells at relative rapidity separations of $\Delta\eta \sim 1\text{--}2$ units can influence each other's transverse momenta. In this way, large momentum correlations at very small $\Delta\eta$ will diffuse to larger rapidity separations, and τ_π controls the rate of this process.

We focus on correlations of transverse momentum fluctuations at two different points in the fluid

$$r(\mathbf{x}_1, \mathbf{x}_2) = \langle \mathbf{g}(\mathbf{x}_1) \mathbf{g}(\mathbf{x}_2) \rangle - \langle \mathbf{g}(\mathbf{x}_1) \rangle \langle \mathbf{g}(\mathbf{x}_2) \rangle. \quad (1)$$

Here, $\mathbf{g} \approx T_{0r} - \langle T_{0r} \rangle$ is the *difference* in transverse momentum density from the global average at position \mathbf{x} . The initial values of both the fluctuations \mathbf{g} and the correlation function (1) are determined at the initial moments of the collisions. We look for correlations (1) that survive through the dynamical evolution, assuming final-state particle momenta are representative of local momentum densities of the fluid at freeze-out.

While shear viscosity diffuses correlations (1) in rapidity, the fluctuation–dissipation theorem states that all dissipative terms are accompanied by stochastic fluctuations due to microscopic interactions. This stochastic noise ensures that even if viscous forces are able to drive the system to equilibrium, stochastic fluctuations would induce random momentum correlations throughout the system. Schematically, including a stochastic term in the stress energy tensor like $T^{\mu\nu} = T_{\text{ideal}}^{\mu\nu} + \Delta T^{\mu\nu} + \text{noise}$ will source correlations in (1), see [1–3].

Additionally, the longitudinal expansion of the medium due to the motion of the colliding nuclei competes with the longitudinal momentum transfer due to shear viscosity. Therefore, we calculate the evolution of correlations following [1] using linearized, second order, Müller–Isreal–Stewart hydrodynamics with noise and one-dimensional longitudinal expansion. Linearized forms of second order equations are discussed in [3–5]. To investigate the evolution of momentum correlations (1), we write the hydrodynamic equations for momentum density rather than velocity. Further, in [1], we show that these evolution equations can also be written for momentum density *fluctuations*. At linear order, shear and longitudinal modes are decoupled, therefore, only shear forces will contribute to the rapidity dependence of (1).

Longitudinal modes may send compression sound waves in the longitudinal direction, however, these modes do not change the positions of fluid cells or relative longitudinal distances between cells. Longitudinal modes also do not transfer any *transverse* momentum between cells.

We distinguish longitudinal and transverse modes using the Helmholtz decomposition. We indicate the divergence free component of the momentum density fluctuation as \mathbf{g} . Now, correlations (1) emerge from only initial state correlations and vortical forces. By keeping only the curl free components of momentum fluctuations, longitudinal modes would modify a similar correlation function. These correlations could be used to study bulk viscosity, sound modes, and thermal and baryon conductivity. We leave this for future work.

Following Ref. [1], we derive a causal diffusion equation for *correlations* of momentum density fluctuation (1) rather than \mathbf{g} itself. If viscosity has enough time, all fluid cells will approach the average value, driving $\mathbf{g} \rightarrow 0$ and $\langle \mathbf{g}(\mathbf{x}_1) \mathbf{g}(\mathbf{x}_2) \rangle \rightarrow \langle \mathbf{g}(\mathbf{x}_1) \rangle \langle \mathbf{g}(\mathbf{x}_2) \rangle$ and, therefore, $r(\mathbf{x}_1, \mathbf{x}_2) \rightarrow 0$. Noise causes random fluctuations — changes of \mathbf{g} — sourcing random correlations in (1). For more information about how correlations emerge from noise, see, for example, Refs. [6–9]. Consequentially, in equilibrium, correlations (1) do not vanish, but approach some value $r \rightarrow r^{\text{eq}}$.

It turns out that the quantity $\Delta r = r - r^{\text{eq}}$ also satisfies the diffusion equation, and we obtain

$$\left[\frac{\tau_\pi}{2} \frac{\partial^2}{\partial \tau^2} + \left(1 + \frac{\kappa \tau_\pi}{\tau} \right) \frac{\partial}{\partial \tau} - \frac{\nu}{\tau^2} \left(2 \frac{\partial^2}{\partial (\Delta \eta)^2} + \frac{1}{2} \frac{\partial^2}{\partial \eta_a^2} \right) \right] \Delta r = 0. \quad (2)$$

We define the relative $\Delta \eta = \eta_1 - \eta_2$ and average $\eta_a = (\eta_1 + \eta_2)/2$ spatial rapidities for pairs of fluid cells at different longitudinal positions. Given the Bjorken expansion, we equate spatial rapidity with rapidity, and τ is the proper time.

Equation (2) describes the causal diffusion of correlations (1) *in excess* of random correlations from noise. We parameterize the shear relaxation time $\tau_\pi = \beta \nu$, where $\nu = \eta/sT$ is the kinematic viscosity, η/s is the shear viscosity to entropy density ratio and T is the temperature. The coefficient β dictates the rate at which signals propagate through the medium and is related to the speed of sound by $c_s = \beta^{-1/2}$. Notice that τ_π scales the time derivatives, and effectively determines the rate at which the correlation function changes.

Three transport coefficients appear in (2), the kinematic viscosity ν , the shear relaxation time τ_π , and finally, the coefficient κ which scales gradients in speeds of fluid cells. For example, in a conformal fluid, where the only scale is T , $\tau_\pi \sim 1/T$, $\eta \sim s \sim T^3$, and $\kappa = 4/3$. In this work, we calculate κ following [10] using the coupled differential equations for causally delayed

heating with the Bjorken flow

$$\frac{ds}{d\tau} + \frac{s}{\tau} = \frac{\Phi}{T\tau}; \quad \frac{d\Phi}{d\tau} = -\frac{1}{\tau_\pi} \left(\Phi - \frac{4\eta}{3\tau} \right) - \frac{\kappa}{\tau} \Phi; \quad \kappa = \frac{1}{2} \left\{ 1 + \frac{d \ln(\tau_\pi/\eta T)}{d \ln \tau} \right\}. \quad (3)$$

Using a parameterization of η/s with T that we take from [11] in combination with (3), we calculate a time dependence of temperature, entropy density, and κ to use in (2).

3. Rapidity correlations

Experimental measurements of two-particle transverse momentum correlations are related to correlations (1) by

$$\mathcal{C} = \langle N \rangle^{-2} \left\langle \sum_i \sum_{j \neq i} p_{t,i} p_{t,j} \right\rangle - \langle p_t \rangle^2 = \langle N \rangle^{-2} \iint \langle \Delta r(\mathbf{x}_1, \mathbf{x}_2) \rangle d\mathbf{x}_1 d\mathbf{x}_2. \quad (4)$$

Here, p_t is the transverse momentum of particle i or j and $\langle \dots \rangle$ is an event average. The STAR experiment has measured (4) differentially as $\mathcal{C}(\Delta\eta, \Delta\phi)$, where $\Delta\eta$ is the relative pseudorapidity and $\Delta\phi$ is the relative azimuthal angle between particle pairs [12, 13]. A differential measurement in $\Delta\phi$ can be used to study the contributions from geometrical fluctuations and we leave this for future work. To eliminate contributions to (1) from geometrical fluctuations, we integrate $\mathcal{C}(\Delta\eta, \Delta\phi)$ over $\Delta\phi$. Since geometrical fluctuations can be characterized by a Fourier cosine series, then the integral of any $\cos(n\Delta\phi)$ on the interval $0 < \Delta\phi < 2\pi$ will vanish. In Fig. 1, STAR integrated $\mathcal{C}(\Delta\eta, \Delta\phi)$ in the region $|\Delta\phi| < 1$.

To find agreement between the measured data in Fig. 1 (red points) and our calculation (solid lines) from (2) and (4), several parameters in (2) must be determined. We use a parameterization of η/s from [11] with (3) to calculate the time dependence of the temperature, kinematic viscosity, and coefficient κ . The best agreement with data results from choices of a formation time of $\tau_0 = 1.05$ fm, a freeze-out temperature of $T_{\text{FO}} = 150$ MeV and $\beta = \tau_\pi/\nu = 5.5$. The value of $\beta = 5.5$ and the non-Gaussian shape of the distribution are our primary results. Importantly, we are able to find similar results in the range of $5 < \beta < 6$, indicating that the data can put realistic constraints on τ_π [14].

In the case of first order ($\beta = 0$) diffusion, the distributions $\mathcal{C}(\Delta\eta)$ are always Gaussian in shape given Gaussian initial conditions. Even with non-Gaussian initial conditions, first order diffusion rapidly drives the distribution to be Gaussian. The STAR measurement of $\mathcal{C}(\Delta\eta)$ in central collisions distinctly shows non-Gaussian shapes that are flatter and even suggest a

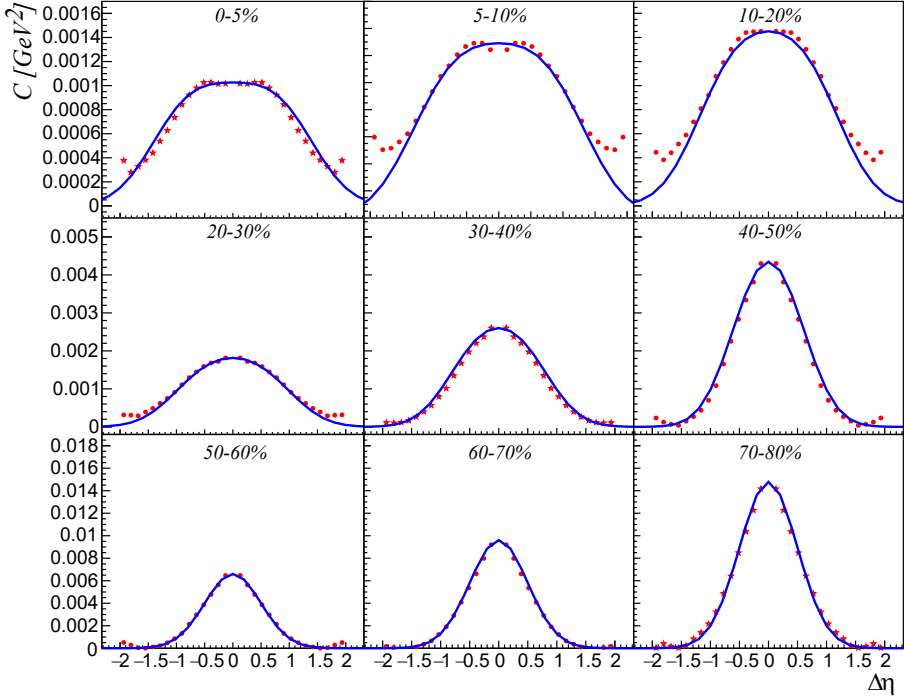


Fig. 1. Relative rapidity distribution of transverse momentum correlations for Au+Au collisions at $\sqrt{s} = 200$ GeV. $\beta = 5.5$, $\tau_0 = 1.05$ fm, $\tau_{f,b=0} = 1.05$ fm, $T_{FO} = 150$ MeV. Data is from the STAR experiment [12].

double peak structure. This indication of a deviation from the $\beta = 0$ case is the motivation for this work. Notice that (2) resembles Telegrapher's equation which has wave and diffusion components. The wave nature of (2) indicates that the initial distribution of Δr will travel as a wave with speed $\beta^{-1/2}$ in Cartesian space. The relative rapidity coordinate system enforces a symmetry, so the initial Δr peak will travel as two oppositely moving peaks. Longitudinal expansion slows the (rapidity) propagation of the peaks by a factor of τ^{-2} . The diffusive nature of (2) acts to produce a diffusion hump that fills the region between the peaks. If freeze-out happens rapidly, the wave pulses will not separate enough to be individually visible. Consequentially, the distribution appears flattened near $\Delta\eta = 0$. The data suggests a dip at $\Delta\eta = 0$ in central collisions which we interpret as the wave pulses separating. It may be possible to resolve the dip with better knowledge of the initial distribution of correlations. We chose the initial width of Δr to match distribution in the most peripheral collisions, but it is likely that the initial distribution is narrower.

3.1. Moments

Examining the moments of the correlation distributions $\mathcal{C}(\Delta\eta)$ is a complementary way of studying the effects of transport coefficients. In [1], we found that the width of $\mathcal{C}(\Delta\eta)$ is most sensitive to the viscosity, but the apparent flattening at $\Delta\eta = 0$ could not be explained with only first order theories of viscous diffusion. Indeed, an earlier work [15] found that the viscosity value itself could be extracted from $\mathcal{C}(\Delta\eta)$ by comparing the width in central collisions to that in peripheral collisions; the STAR experiment measured (1) in [12] for this reason and subsequently found the flattening of $\mathcal{C}(\Delta\eta)$ in central collisions.

In Fig. 2, we show the centrality dependence of the root-mean-square (RMS) width of the distributions shown in Fig. 1. STAR data is from [12] and the error band is representative of their estimates of the uncertainty due to their fitting procedure.

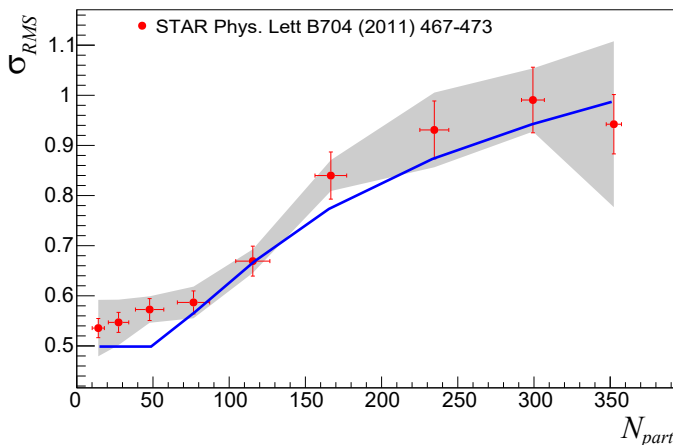


Fig. 2. RMS width of $\mathcal{C}(\Delta\eta)$ from Fig. 1 versus N_{part} . Data points are from [12]. Error bands on the data represent uncertainty in the experimental fitting procedure to the experimental points from Fig. 1. The solid line is the theoretical comparison calculated from the theoretical distributions in Fig. 1.

The width of $\mathcal{C}(\Delta\eta)$ indicates very little about the non-Gaussian shape of the distribution. To address this, we look at higher moments, namely the kurtosis. Recall that for any random variable ξ , the first moment is the average, $\langle \xi \rangle$, and second moment is the variance $\sigma^2 = \langle (\xi - \langle \xi \rangle)^2 \rangle$. All higher central moments are calculated similarly as $\langle (\xi - \langle \xi \rangle)^n \rangle$ with integer n indicating the n^{th} moment. So-called standardized moments take the form of $\langle (\xi - \langle \xi \rangle)^n \rangle / \sigma^n$. Given a distribution that is symmetric about zero, the average is zero $\langle \xi \rangle = 0$ and then $\sigma^2 = \langle \xi^2 \rangle$, and is related to the RMS

width by $\sigma_{\text{RMS}} = \sqrt{\langle \xi^2 \rangle}$. Additionally for symmetric distributions, the third moment, known as the skewness, is also zero. The fourth moment, known as the (excess) kurtosis $\langle (\xi - \langle \xi \rangle)^4 \rangle / \sigma^4 - 3$, may illuminate features of $\mathcal{C}(\Delta\eta)$, that the width may not. For Gaussian distributions, the kurtosis is zero. Compared to the Gaussian, distributions that are more sharply peaked or have more rapidly decreasing tails will have a positive kurtosis. For distributions with a flatter peak or more slowly decreasing tails, the kurtosis will be negative.

Figure 3 shows the kurtosis of distributions in Fig. 1 as a function of centrality. Notice that the values are mostly negative, indicating a flatter peak and/or broader tails in comparison to a Gaussian shape. To highlight the importance of the distribution tails, compare in Fig. 3 the kurtosis of the calculated $\mathcal{C}(\Delta\eta)$ with tails extending to infinity (solid line) to the kurtosis calculated in the range of the data (dashed line). The open circles represent our extraction of the kurtosis from the STAR data in Fig. 1 in the range of $\Delta\eta < 1.55$. Cutting off the tails of the distribution artificially lowers the kurtosis, but the solid line still shows a significant negative kurtosis in central collisions where the second order diffusive effects are most noticeable. We are working to develop a method for extracting transport coefficients from moments of the data for more direct experimental use. This work is in progress.

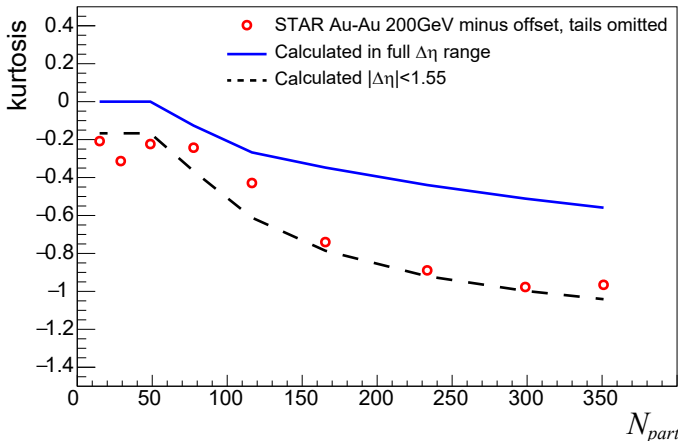


Fig. 3. Kurtosis of $\mathcal{C}(\Delta\eta)$ from Fig. 1 versus N_{part} . We extract the open circles from experimental data in Fig. 1 in the range of $\Delta\eta < 1.55$. The dashed line represents the kurtosis calculated from theoretical values Fig. 1 in the same rapidity range. The solid line is the theoretical kurtosis calculated including the tails of the distribution.

Additionally, the kurtosis appears also useful as a theoretical tool. Figure 4 shows the kurtosis for each centrality plotted as a function of time. For all centralities, we take the initial values of Δr to have a distribution matching the most peripheral collisions (70–80% centrality in Fig. 1) and assume those collisions have no diffusion. The shape of this distribution is Gaussian and, therefore, has zero kurtosis. In more central collisions, these initial correlations then spread following the wave and diffusive nature of (2). The initial peak separates into two separate peaks moving away from each other with a speed $\beta^{-1/2}$ in Cartesian coordinates. In relative rapidity coordinates, this separation is modified due to longitudinal expansion. Figure 4 indicates that peak separation happens quickly. In the first 2 fm/c, the kurtosis drops rapidly as the $\Delta\eta = 0$ part of the distribution becomes flatter due to the peak separation. As the system evolves, the longitudinal expansion practically freezes the peaks in place in relative rapidity and, therefore, the kurtosis changes slowly, while viscosity attenuates correlations driving them toward a more Gaussian shape. Notice that even the comparatively long-lived central collisions develop most of their non-Gaussian rapidity structure in the early moments — during the QGP phase.

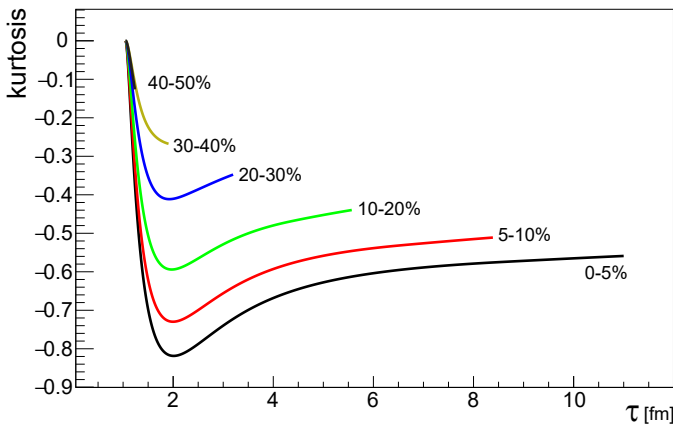


Fig. 4. Kurtosis of $\mathcal{C}(\Delta\eta)$ from Fig. 1 versus time for select centralities. The rapid drop at early times corresponds to wave-like propagation of correlations dictated by (2). Endpoints of each centrality curve match the value of the solid line in Fig. 3 at the same centrality.

4. Conclusion

Transport coefficients such as the viscosity ν or the shear relaxation time $\tau_\pi = \beta\nu$ are characteristic quantities that dictate how a dynamic medium transitions from an initially anisotropic state toward an equilibrated state. Viscosity dictates how fluctuations in the fluid are driven toward equilibrium

and the relaxation time controls the rate at which this process acts. While experiments have developed several techniques and observables to constrain estimates of the viscosity, very little has been done to constrain values of τ_π . In this work, we argue that τ_π can be estimated from the rapidity dependence of two-particle momentum correlations (4). We find good agreement with data using $\beta = \tau_\pi/\nu = 5.5$, where $\nu = \eta/sT$ is the kinematic viscosity. Significantly, we obtain comparable results using the range of $5 < \beta < 6$ [14]. This indicates that the data can indeed be used to put realistic limits on the value of τ_π .

We interpret the shape of the relative rapidity distribution of transverse momentum correlations $\mathcal{C}(\Delta\eta)$, Fig. 1, with a causal diffusion equation (2) that describes the evolution of correlations (1) in excess of correlations induced by stochastic noise [1, 14]. By examining (1), we see not only that causality is enforced by the relaxation time which scales time derivatives, but also that correlations spread in relative rapidity like wave pulses with speed $\beta^{-1/2}$. The separation of these wave pulses explains the flattening of the peak of $\mathcal{C}(\Delta\eta)$ in central collisions.

Our diffusion equation (2) was derived considering only longitudinal flow, but to achieve the typical initial temperatures at RHIC, 1+1D hydrodynamics requires longer lifetimes than 3+1D models. This may bias our current result and we will address this issue in future work. Our values of β agree with kinetic theory predictions $\beta = 5$. Calculations from scalar field theory suggest $5 < \beta < 7$ [16], which is also in agreement with our estimate. Using AdS/CFT values like $\beta = 1.23$, we are not able to obtain agreement with data in Fig. 1 using reasonable parameters.

We also study the moments of the distributions $\mathcal{C}(\Delta\eta)$ with the ambition of making estimations of transport coefficients more experimentally accessible. We show the centrality dependence of the RMS width and the kurtosis of $\mathcal{C}(\Delta\eta)$ in Figs. 2 and 3, respectively. We argue that the width is most sensitive to the viscosity but not the relaxation time, however, the kurtosis is indeed very sensitive to the relaxation time. The most central collisions that most clearly demonstrate the wave nature of (1), correspondingly have the most negative kurtosis.

A significant benefit of this work is the development of evolution equations like (2) for *correlations* rather than point-by-point densities on a grid. In contrast to hydrodynamic or transport simulations *e.g.* [3, 17, 18], that have computationally expensive numerics and lose two-particle spatial correlation information when performing freeze-out, we map the evolution of correlations throughout the whole lifetime of the collision with comparably small numerical resources. Finally, we comment that more information can be obtained about two-particle correlation functions by studying pre-equilibrium fluctuations [19].

REFERENCES

- [1] S. Gavin, G. Moschelli, C. Zin, *Phys. Rev. C* **94**, 024921 (2016).
- [2] J.I. Kapusta, B. Müller, M. Stephanov, *Phys. Rev. C* **85**, 054906 (2012).
- [3] C. Young *et al.*, *Phys. Rev. C* **91**, 044901 (2015).
- [4] P. Romatschke, *Int. J. Mod. Phys. E* **19**, 1 (2010).
- [5] J.I. Kapusta, C. Plumberg, *Phys. Rev. C* **97**, 014906 (2018).
- [6] S. Pratt, C. Young, *Phys. Rev. C* **95**, 054901 (2017).
- [7] S. Pratt, *Phys. Rev. C* **96**, 044903 (2017).
- [8] Y. Akamatsu, A. Mazeliauskas, D. Teaney, *Nucl. Phys. A* **967**, 872 (2017).
- [9] Y. Akamatsu, A. Mazeliauskas, D. Teaney, *Phys. Rev. C* **95**, 014909 (2017).
- [10] A. Muronga, *Phys. Rev. Lett.* **88**, 062302 (2002) [*Erratum ibid.* **89**, 159901 (2002)].
- [11] H. Niemi *et al.*, *Phys. Rev. C* **86**, 014909 (2012).
- [12] H. Agakishiev *et al.*, *Phys. Lett. B* **704**, 467 (2011).
- [13] M. Sharma, C.A. Pruneau, *Phys. Rev. C* **79**, 024905 (2009).
- [14] G. Moschelli, S. Gavin, *Nucl. Phys. A* **982**, 311 (2019).
- [15] S. Gavin, M. Abdel-Aziz, *Phys. Rev. Lett.* **97**, 162302 (2006).
- [16] A. Czajka, S. Jeon, *Phys. Rev. C* **95**, 064906 (2017).
- [17] L. Yan, H. Grönqvist, *J. High Energy Phys.* **1603**, 121 (2016).
- [18] K. Nagai, R. Kurita, K. Murase, T. Hirano, *Nucl. Phys. A* **956**, 781 (2016).
- [19] S. Gavin, G. Moschelli, C. Zin, *Phys. Rev. C* **95**, 064901 (2017).